SCCI조건에서의 희박 정상-헵탄/공기 혼합물의 점화에 관한 직접수치모사: 화학적 측면

유광현* · Minh Bau Luong* · 유춘상*†

DNSs of the Ignition of a Lean *n*-Heptane/Air Mixture under SCCI Conditions: Chemical Aspects

Gwang Hyeon Yu*, Minh Bau Luong*, Chun Sang Yoo*†

ABSTRACT

The chemical aspects of thermally- and/or compositionally-stratified *n*-heptane/air mixture under HCCI conditions are examined to obtain the insight of the ignition process in HCCI combustion. Chemical explosive mode analysis (CEMA) is adopted to understand the spatial ignition characteristics of the lean *n*-heptane/air mixture by identifying controlling species and elementary reactions at different locations and times.

Key Words: DNS, HCCI, SCCI, chemical explosive mode analysis (CEMA)

The overall reaction pathways of *n*-heptane oxidation relevant to HCCI combustion are discussed. As shown in Fig. 1, the low-temperature chemistry (LTC) of *n*-heptane oxidation is first initiated by the H-atom abstraction from a fuel molecule, RH, reacting with molecular oxygen (RH + O_2 → R + HO_2). As such, HO_2 increases significantly as a result of rapid *n*-heptane decomposition during the first-stage ignition. Alkyl radical, R, then reacts with O_2 to produce alkylperoxy radical, RO_2, via R + O_2 + M → RO_2 + M. The rate of addition of O_2 to alkyl radical and its equilibrium depend strongly on p, T, and ϕ and hence, the temperature threshold for separating the low-and high-temperature reaction path varies depending on specific conditions. Next, RO_2 radical isomerization occurs to form hydroperoxyalkyl, QOOH, (RO_2 → QOOH) followed by another O_2 addition (QOOH + O_2 → O_2QOOH). The overall rate of the LTC is primarily controlled by the rate of chain branching reactions through the production and decomposition of keto-hydroperoxide, KOOH; O_2QOOH → KOOH + OH and KOOH → OH + KO.

The low-temperature reaction cycle is suppressed when temperature exceeds a critical value at which the competing reaction (R + O_2 → olefin + HO_2) terminates the first-stage ignition. Between the first-and second-stage ignitions, the intermediate-temperature chemistry (ITC), which is actually the combination of the low-and high-temperature chemistries, dominates the ignition of n-heptane/air mixture; alkyl radical and hydroperoxyalkyl species convert into the other fuel species (e.g., cyclic ether species, olefins, and ketens) plus OH and HO_2. In this period, the rate of temperature increases is significantly reduced due to a lower reactivity of the system. Over a certain temperature threshold, the chain branching reaction of hydrogen peroxide (H_2O_2 + M → OH + OH + M) becomes highly reactive, resulting in large enough temperature increase to initiate the chain branching reactions at high temperatures,

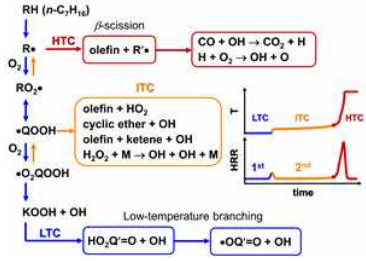

Fig. 1 Schematic of reaction pathways

* 유니스트 기계공학과
† 연락저자, csyoo@unist.ac.kr
TEL : (052)217-2322 FAX : (052)217-2309

controlled by H + O_2 → O + OH. At this point, high-temperature chemistry (HTC) becomes predominant over the LTC and the second-stage ignition starts to occur. HTC of *n*-heptane oxidation can be simply understood as a process of sequential decomposition of large fuel species to small radicals, down to CH_2O, CHO, H_2O_2, HO_2, and CO. At the final stage of the ignition, therefore, reaction pathways involve the core of H_2/CO oxidation mechanism.

Based on the above discussion, the temporal evolution of the mean mass fraction of important species (e.g., n-C_7H_{16}, HO_2, H_2O_2, OH, CO, and CO_2) and the mean HRR is shown in Figs. 2-4. Three distinct behaviors of the species are readily observed from the figures depending on T_0. First, for Cases 4 and 11, almost all *n*-heptane is rapidly consumed by the LTC (RH + O_2 → R + HO_2) and as such, HO_2 mass fraction increases significantly and has its first peak during the first-stage ignition, which is similar to their corresponding 0-D case with T_0 = 805 K. Since T' for Cases 4 and 11 are relatively small compared to those of other cases (Cases 2, 14, and 21), the overall combustion proceeds similarly to their corresponding 0-D ignition during the first-stage of ignition; however, for Cases 2, 14, and 21 with relatively large T', the wide span of the first-stage ignition delay in the initial mixture results in the gradual reduction of *n*-heptane and increment of HO_2, which is manifested in the relatively-small and temporally-distributed HRR during the early stage of the ignition. In either case, however, the temporal spread of HRR (Cases 2, 4, and 21) during the second-stage ignition is manifested in a gradual increase of OH and decrease of H_2O_2 as HTC dominates the overall combustion, implying that the overall combustion occurs not only by the spontaneous auto-ignition mode but also by the deflagration mode of combustion.

Second, for cases with T_0 = 933 K, only a small fraction of *n*-heptane is rapidly consumed during the first-stage ignition and then, it decreases linearly until the end of combustion. Since the HRR from the first-stage ignition at T_0 = 933 K is much smaller than at T_0 = 805 K, the consumption of

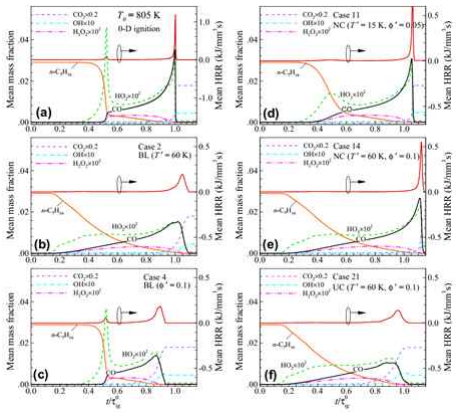

Fig. 2 Temporal evolutions of the mean mass fractions of important species and mean HRR at T_0 = 805 K

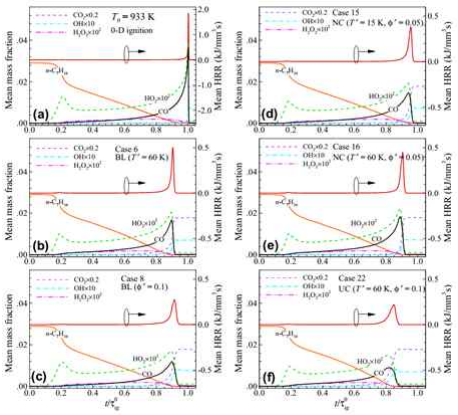

Fig. 3 Temporal evolutions of the mean mass fractions of important species and mean HRR at T_0 = 933 K

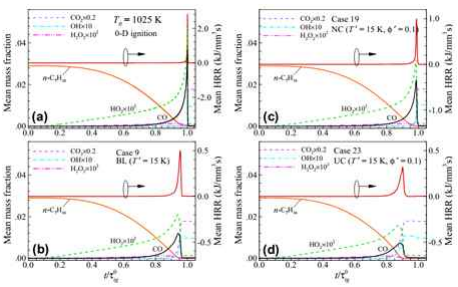

Fig. 4 Temporal evolutions of the mean mass fractions of important species and mean HRR at T_0 = 1025 K

n-heptane for cases with T_0 = 933 K during the first-stage ignition becomes smaller. For all cases with T_0 = 933 K, HO_2 has two peaks at the first- and second-stage ignition;

the first peak occurs through RH + O_2 → R + HO_2 and the second is attributed to the accumulation of HO_2 via R + O_2 → olefin + HO_2 of ITC. The temporal distribution of the mean HRR during the second-stage ignition is manifested in the progressive increase of OH and reduction of H_2O_2.

Third, for cases with T_0 = 1025 K, *n*-heptane is first gradually consumed and then, the consumption rate keeps increasing till the end of the overall combustion. At high T_0 of 1025 K, there is no first-stage ignition and the intermediate-to-high temperature chemistries govern the ignition such that the consumption of *n*-heptane and accumulation of HO_2 occurs gradually through the ITC as shown in Fig. 4. As deflagrations developed from ignition kernels propagate into unburnt mixture, significant heat release starts to occur and CO and OH levels increase rapidly. At the final stage, the unburnt mixture is consumed primarily by the spontaneous auto-ignition and as such, the mass fraction of CO and HO_2 decreases rapidly. It is also of interest to note that the level of H_2O_2 concentration is relatively low compared to that at T_0 = 805 and 933 K. At high temperature, H_2O_2 decomposes rapidly into OH via H_2O_2 + M → OH + OH + M and as such, remains relatively constant till the thermal ignition.

Details of CEMA formation can be found in [2-3]. Figure 5 shows the isocontours of HRR, temperature, $Y_{n\text{-}c7H16}$, the log-scale of Re (λ_e), and the EI values of important species which exhibit relatively-large EI values for Case 16 at t/τ_{ig}^0 = 0.67. Two points are to be noted from the figure. First, it is readily observed from Fig. 5a-d that mixture with Re (λ_e) < 0 is already burned while the ignition of mixture with Re(λ_e) > 0 is still underway. In between the two distinct regions, there exist thin deflagrations with large HRR and $Da_c \sim O(1)$. Second, temperature, n-heptane, and H_2O_2 are the main species that render the mixture to be explosive in the unburnt region. More specifically, temperature and n-heptane are the main source of the CEM at relatively-low temperature region (T~1000 K) while H_2O_2 becomes important for the ignition of unburnt mixture at relatively-high temperature region (T~1100 K). This is because fuel decomposition still occurs at the relatively-low temperature region with large fuel concentration. At T~1100 K, however, the chain-branching reaction of H_2O_2 becomes highly reactive, which subsequently results in initiating high temperature chemistry. CO and OH are also found to be the most important species in the burnt region, in which the HTC remains controlling the combustion process. From 1-D profiles of key species and their EI values (not shown here), from upstream to downstream through deflagrations, EI(CO) increases nearly up to unity while EI(T) and EI(H_2O_2) vanish rapidly, which is consistent with the characteristics of n-heptane oxidation observed in freely-propagating premixed flames and auto-ignition.

Fig. 6. shows critical reactions involving the important EI species. Note that Fig. 6f shows the cumulative PI value of R293-R300: RH + (OH, HO_2) → R + (H_2O, H_2O_2). It is generally believed that CO + OH → CO_2 + H (R7) and H + O_2 → O + OH (R8) are the two most important reactions in a hydrocarbon/air combustion process regardless of specific fuel type. In this study, both reactions are also found to be important to the CEM especially across the deflagrations. This is primarily because R7 is the main conversion path of CO to CO_2 and R8 is the most important chain-branching reaction at high temperature. In addition, HO_2 formation reaction, H + O_2 + M → HO_2 + M (R24), is also found to be important at the deflagrations because it is one of the most exothermic reactions in hydrogen/air premixed flames.

In the unburnt region upstream of the deflagrations (Figs. 6e-f), however, it is readily observed that the chain branching of H_2O_2 (R48) and the generation of alkyl radical and H_2O_2 (R292-R300) are the most important reactions to the CEM. Consistent with the EI analysis above, the conversion of fuel to alkyl radical and H_2O_2 is important for unburnt mixtures with T~1000 K and relatively-high fuel concentration; however, the chain branching reaction of H_2O_2 becomes more important at T~1100 K. The result implies that H_2O_2 generated from fuel decomposition reactions becomes reactive at relatively-high

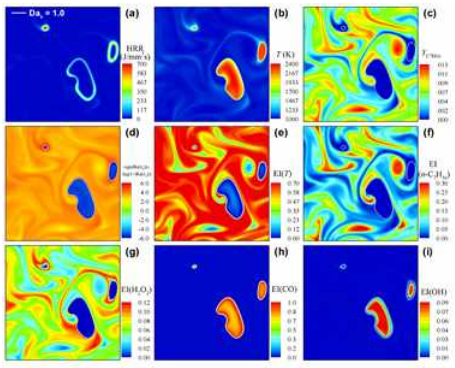

Fig. 5 Isocontours of (a) HRR, (b) temperature, (c) Y_{C7H16}, (d) sign(Re(λe))×log(1+|Re(λe|)), and EIs for Case 16 at t/τ_{ig} = 0.67.

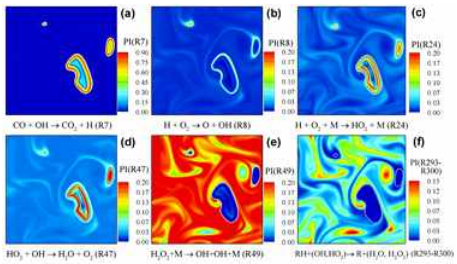

Fig. 6 Isocontours of PIs of controlling reactions for Case 16 at t/τ_{ig} = 0.67.

temperature region, subsequently inducing the thermal ignition of the unburnt mixtures.

The same EI and PI analyses are applied to Case 16 at the maximum HRR (not shown here). Even thin deflagrations with high HRR are readily observed-these characteristics are similar to early nascent deflagrations in terms of EI and PI values. However, significant heat is released upstream of the deflagrations by the thermal ignition of unburnt mixtures, which is manifested in large EI values of temperature together with relatively-small EI values of H_2O_2 and non-zero EI values of OH. The occurrence of thermal ignition in the unburnt region is also manifested in relatively-large PI values of high temperature chain branching reaction (R8) and HO_2 formation/consumption reactions (R24 and R47). Because of high temperature of the unburnt mixtures, 1200-1600 K, the HTC starts overwhelming the ITC; R8 becomes more important to CEM than H_2O_2 decomposition reaction (R49).

The chemical aspects of the ignition of thermally-and/or compositionally-stratified lean *n*-heptane/air mixture under HCCI conditions were investigated using CEMA. In regions where the spontaneous auto-ignition mode of combustion is predominant, temperature, H_2O_2, and *n*-heptane are identified as the key species for the CEM prior to thermal ignition while the chain branching reaction of H_2O_2 and the conversion reaction of n-heptane to alkyl radical and H_2O_2 are the main reactions of the ITC. During thermal ignition, however, temperature is found to be the predominant species and high-temperature reactions represented by H + O_2 → O + OH are responsible for the thermal ignition. At deflagrations, temperature, CO, and OH are the most important species while the conversion reaction of CO to CO_2 and high-temperature chain branching reaction of H + O_2 → O + OH are identified to be important to the CEM.

Acknowledgements

The work was supported by the 2015 Research Fund (1.150033.01) of Ulsan National Institute of Science and Technology (UNIST). MBL and KHY were also supported by BK21Plus funded by the Ministry of Education. This research used the resources of the KAUST Supercomputing Laboratory.

References

[1] M.B. Luong, G.H. Yu, T. Lu, S.H. Chung, C.S. Yoo, submitted to Combust. Flame
[2] T.F. Lu, C.S. Yoo, J.H. Chen, C.K. Law, J.F.M. 652 (2010) 45-64.
[3] R. Shan, C.S. Yoo, J.H. Chen, T. Lu, Combust. Flame, 159 (2012) 3119-3127.
[4] Z. Luo, C.S. Yoo, E.S. Richardson, J.H. Chen, C.K. Law, T. Lu, Combust. Flame, 159 (2012) 265-274
[5] C.S. Yoo, T. Lu, J.H. Chen, and C.K. Law, Combust. Flame 158 (2011) 1727-1741.
[6] M.B. Luong, Z. Luo, T. Lu, S.H. Chung, C.S. Yoo, Combust. Flame, 160 (2013) 2038-2047.
[7] M.B. Luong, T. Lu, S.H. Chung, C.S. Yoo, Combust. Flame 161 (2014) 2878-2889.
[8] S.O. Kim, M.B. Luong, J.H. Chen, C.S. Yoo, Combust. Flame 162 (2015) 717-726.